Mon. Not. R. Astron. Soc. **000**, 1–5 (2012) Printed 22 November 2012 (MN LATEX style file v2.2)

ALMA and VLA observations of the outflows in IRAS 16293–2422

Laurent Loinard[1,2], Luis A. Zapata[1], Luis F. Rodríguez[1], Gerardo Pech[1], Claire J. Chandler[3], Crystal L., Brogan[4], David J. Wilner[5], Paul T.P. Ho[5,6], Bérengère Parise[2], Lee W. Hartmann[7], Zhaohuan Zhu[8], Satoko Takahashi[6], and Alfonso Trejo[6]

[1]*Centro de Radiostronomía y Astrofísica, Universidad Nacional Autónoma de México, 58089 Morelia, Michoacán, México*
[2]*Max-Planck-Institut für Radioastronomie, Auf dem Hügel 69, 53121 Bonn, Germany*
[3]*National Radio Astronomy Observatory, P.O. Box O, Socorro, NM 87801*
[4]*National Radio Astronomy Observatory, 520 Edgemont Road, Charlottesville, VA 22903-2475*
[5]*Harvard-Smithsonian Center for Astrophysics, 60 Garden Street, Cambridge, MA 02138*
[6]*Academia Sinica Institute of Astronomy and Astrophysics, Taipei, Taiwan*
[7]*Department of Astronomy, University of Michigan, 500 Church St., Ann Arbor, MI 48109, USA*
[8]*Department of Astrophysical Sciences, 4 Ivy Lane, Peyton Hall, Princeton University, Princeton, NJ 08544*

Accepted 22 November 2012. Received 22 November 2012; in original form 22 November 2012

ABSTRACT

We present ALMA and VLA observations of the molecular and ionized gas at 0.1-0.3″ resolution in the Class 0 protostellar system IRAS 16293-2422. These data clarify the origins of the protostellar outflows from the deeply embedded sources in this complex region. Source A2 is confirmed to be at the origin of the well known large scale north-east–south-west flow. The most recent VLA observations reveal a new ejection from that protostar, demonstrating that it drives an episodic jet. The central compact part of the other known large scale flow in the system, oriented roughly east-west, is well delineated by the CO(6-5) emission imaged with ALMA and is confirmed to be driven from within component A. Finally, a one-sided blueshifted bubble-like outflow structure is detected here for the first time from source B to the north-west of the system. Its very short dynamical timescale ($\sim$ 200 yr), low velocity, and moderate collimation support the idea that source B is the youngest object in the system, and possibly one of the youngest protostars known.

Key words: stars: formation — ISM: jets and outflows — stars: individual (IRAS 16293-2422) — techniques: interferometric — submillimeter

1 INTRODUCTION

Outflows constitute one of the most spectacular, emblematic, and relevant early manifestations of the star formation process (e.g. Lada 1985; Arce et al. 2007). By removing angular momentum, they allow accretion to proceed (Bodenheimer 1995), and through their injection of mechanical energy, they can affect the overall evolution of star-forming regions (Reipurth et al. 1997). Their morphologies can also provide clues on the properties of the driving sources. For instance, the degree of collimation of outflows is believed to correlate with the age and mass of the driving protostars (Machida et al. 2008; Arce et al. 2007), while multipolar outflows are often an indication that the central engine is a multiple system (e.g. Carrasco-González et al. 2008).

IRAS 16293–2422 (Ceccarelli et al. 2000; Crimier et al. 2010) is located at a distance of 120 pc (Loinard et al. 2008) in the eastern part of the Ophiuchus complex. Soon after its discovery (Walker et al. 1986), it was found to power two bipolar outflow structures (Mizuno et al. 1990). One is oriented in the north-east–south-west direction (at a position angle of about 55° and hereafter called the NE-SW flow), while the other is oriented nearly east-west (P.A. $\sim$ 110°, hereafter the EW flow). The existence of at least two protostellar sources was also established early thanks to high resolution radio observations (Wootten 1989, Mundy et al. 1992). These objects are known as component A to the south-east, and component B to the north-west, and their projected separation is about 5″ (Figure 1). While component B remains single even at the highest angular resolution available ($\sim$ 0.05 arcsec; Rodríguez et al. 2005; Chandler et al. 2005), component A breaks up into two centimeter sub-components called A1 and A2 at resolutions better than about 0.2″ (Figure 1). Because the relative orientation of the A1/A2 pair at the time of its discovery was very similar to the direction of the NE-SW flow, A1 was initially believed to be an ejecta from A2. However, analysis of the relative motion of A1 and A2 favors a scenario where these two sources trace the two stars in a binary system (Loinard 2002; Chandler et al. 2005; Loinard et al. 2007, Pech et al. 2010). Sub-arcsecond submillimeter continuum observations obtained with the SMA (Submillimeter Array) revealed additional structure in component A (Chandler et al. 2005). While the emission is dominated by a bright compact source (called Aa) centered

almost exactly between A1 and A2, an additional source (Ab) was detected to the north-east of component A (Figure 1). This source has not been detected at any other wavelengths so far, and its exact nature remains mysterious.

The NE-SW outflow has long been known to originate in component A (e.g. Hirano et al. 2001; Castets et al. 2001). This association was unambiguously confirmed, and was further constrained, when Loinard et al. (2007) witnessed, at radio wavelengths, the ejection from A2 of a bipolar system of ejecta which, subsequently, moved away from A2 roughly along the direction of the NE-SW flow (Pech et al. 2010). The EW flow was recently shown to also originate from within component A by Yeh et al. (2008) who presented SMA CO(2-1) and CO(3-2) observations at an angular resolution of a few arcseconds. These SMA data, however, have insufficient angular resolution to distinguish between A1 and A2 as the driving source for the EW flow. Interestingly, there is little evidence for outflow activity from component B. Jørgensen et al. (2011) have presented submillimeter (SMA) observations of IRAS 16293–2422 that resolve the A and B components and do not show strong indications for high velocity gas toward B. Yeh et al. (2008) reported the detection of a compact blue-shifted CO structure to the south-east of source B (their structure b2), but their data was insufficient to decide whether or not this was a compact flow from source B. Rao et al. (2009) also detected this structure, and argued that it was part of an additional outflow driven by source A and oriented at a position angle of about 145°. In this *Letter*, we present combined ALMA (Atacama Large Millimeter/submillimeter Array) and VLA (Karl G. Jansky Very Large Array) observations of IRAS 16293–2422 that help elucidate the origin and nature of the outflows in this complex young stellar system.

2 OBSERVATIONS

2.1 ALMA data

IRAS 16293–2422 was observed at λ = 0.45 mm with fifteen 12-m antennas of ALMA on April 2012, during the science verification data program. The 105 independent baselines ranged in projected length from 26 to 403 m. The primary beam of ALMA at 0.45 mm has a FWHM of 8″, so the observations were made in mosaicking mode with half-power point spacing between field centers to cover both source A and source B. The digital correlator was configured in 4 spectral windows of 1875 MHz and 3840 channels each. This provides a channel spacing of 0.488 MHz ($\sim$ 0.2 km s^{-1}) per channel, but the spectral resolution is a factor of two lower (0.4 km s^{-1}) due to online Hanning smoothing. Observations of Juno provided the absolute scale for the flux density calibration while observations of the quasars J1625–254 and NRAO530 (with flux densities of 0.4 and 0.6 Jy, respectively) provide the gain calibration. The quasars 3C279 and J1924-292 were used for the bandpass calibration. The data were calibrated, imaged, and analyzed using the Common Astronomy Software Applications (CASA) and KARMA software (Gooch 1996). The continuum emission as well as many spectral lines were detected in these ALMA data (see Jørgensen et al. 2012). Here we concentrate on the analysis of the continuum emission and of the CO(J=6-5; ν=0) at a rest frequency of 691.47308 GHz. The r.m.s. noise, measured in line-free channels on either side of the CO line, is about 50 mJy beam^{-1} at an angular resolution of 0.″32 × 0.″18; –69°. Only a small number of line-free channels were averaged to calculate the continuum, so the r.m.s. noise of the continuum image is only moderately better (20 mJy beam^{-1}) than that in the individual spectral channels.

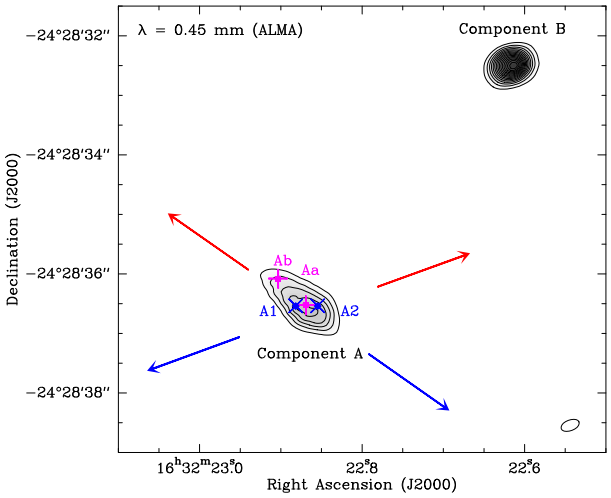

Figure 1. Sub-millimeter continuum image of the IRAS 16293–2422 system from ALMA. The contours run from 0.2 to 4 Jy beam^{-1} by steps of 0.2 Jy beam^{-1}; the synthesized beam (0.″32 × 0.″18; –69°) is shown at the bottom-right. The noise level is 0.02 mJy beam^{-1}. The two main components (A and B) are labelled, and the direction of the two outflows driven from component A are indicated (from Mizuno et al. 1990). The submillimeter peaks Aa and Ab from Chandler et al. (2005) and the centimeter sources A1 and A2 are shown.

2.2 VLA data

IRAS 16293–2422 was observed with the VLA in its most extended (A) configuration on 2011, June 5 and 8 at λ = 7 mm, and on 2011, August 12 at λ = 4 cm. In all cases, the absolute flux calibrator was 3C286 (J1331+3030), while the amplitude and phase gains were monitored using observations of J1625–2527. At 7 mm, sixteen contiguous spectral windows, each containing 64 spectral channels 2 MHz-wide were recorded simultaneously to produce a total bandwidth of 2 GHz (between 40 and 42 GHz). At 4 cm, eight contiguous spectral windows, each containing 64 spectral channels 2 MHz-wide were recorded simultaneously to produce a total bandwidth of 1 GHz (between 6.8 and 7.8 GHz).[1] The data calibration was performed using the CASA software. The data were manually inspected and flagged, and calibrated following standard procedures. The calibrated visibilities at 4 cm were imaged using a nearly uniform weighting scheme (Robust parameter set to –2 in CASA) yielding a synthesized beam of 0.″44 × 0.″16; –11° and a noise level of 16 μJy beam^{-1}. The visibilities at 7 mm were imaged both with natural weighting (Robust = +2) to obtain the highest sensitivity (at the detriment of angular resolution), and with intermediate weighting (Robust = 0) to obtain higher angular resolution (at the detriment of sensitivity). The synthesized beam was 0.″14 × 0.″12; +69° and the sensitivity was 19 μJy beam^{-1} in the former case, while they were 0.″08 × 0.″07; –35° and 31 μJy beam^{-1} in the latter. While the sensitivity at 4 cm is near the theoretically expected value given the integration time, the sensitivity at 7 mm is about 50% worse than expected. Additional analysis will be needed to understand the origin of this degradation, but we note that in spite of this effect, the maps presented here are roughly 5 times deeper that the best previous 7 mm images (Rodríguez et al. 2005).

[1] A second spectral band, corresponding to the frequency range from 4.2 to 5.2 GHz was observed simultaneously with the 4 cm data presented here, but will not be discussed in this *Letter*.

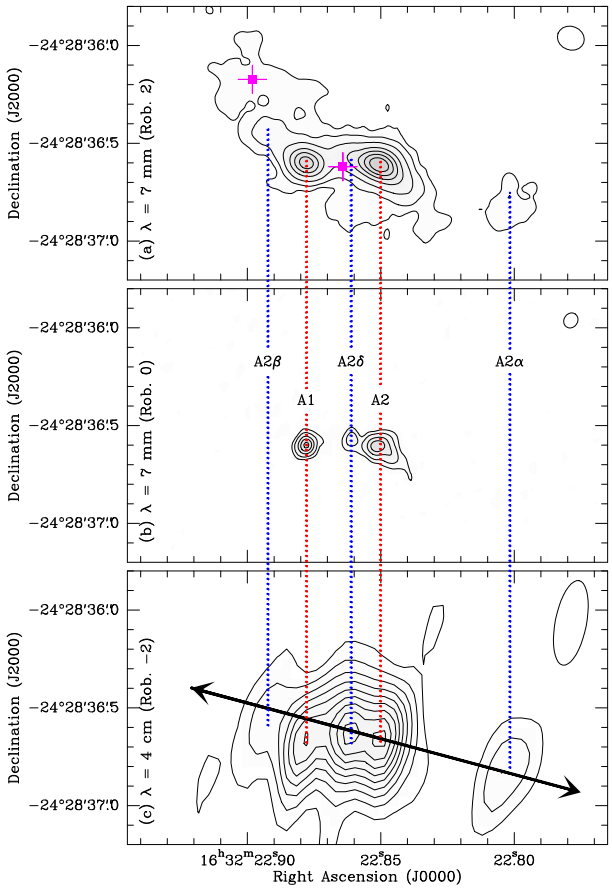

Figure 2. VLA continuum images of IRAS 16293–2422. (a) 7 mm image reconstructed with natural weighting to optimize sensitivity. The synthesized beam (0.″14 × 0.″12; +69°) is shown at the top-right of the panel, and the sensitivity is 19 μJy beam^{-1}. The contours are at 70, 140, 300, 600, 900, etc. μJy beam^{-1}. For reference, the position of the sub-millimeter peaks Aa and Ab are shown as magenta crosses. Note the faint extension to the NE coincident with Ab and the extension of the sub-millimeter ALMA image, and the faint emission associated with the ejecta A2α and A2β. (b) 7 mm image reconstructed with intermediate weighting. The synthesized beam (0.″08 × 0.″07; −35°) is shown at the top-right of the panel, and the sensitivity is 31 μJy beam^{-1}. The contours are at 150, 300, 600, 900, etc. μJy beam^{-1}. Note the new ejecta A2δ. (c) 4 cm image where all the sources and ejecta are seen. The synthesized beam (0.″44 × 0.″16; −11°) is shown at the top-right of the panel, and the sensitivity is 16 μJy beam^{-1}. The first contour and the contour spacing are at μJy beam^{-1}. The double arrow shows the direction (at P.A. 70°) along which the ejecta A2α, A2β, and A2δ were launched.

3 RESULTS AND DISCUSSION

3.1 Continuum emission and the NE-SW flow

The sub-millimeter continuum emission (λ = 0.45 mm) measured by ALMA reveals the usual double source structure of IRAS 16293–2422 (Figure 1). Component B is resolved but compact, with a peak brightness temperature of about 160 K. The total flux measured here with ALMA ($\sim$ 12.2 Jy) is consistent with the trend observed at lower frequencies that the spectral index of source B is between 2 and 2.5 from centimeter to submillimeter wavelengths (Chandler et al. 2005). Component A is elongated along the NE-SW direction, with its peak at the position of source Aa, and the faint extension to the NE corresponding to the position of source Ab reported by Chandler et al. (2005). Interestingly, the centimeter sub-components A1 and A2 are not identifiable in this image, although the angular resolution would be sufficient to separate them. The peak brightness temperature of the sub-millimeter emission in component A is about 30 K. The overall properties of the ALMA image of component A suggest that the sub-millimeter continuum is dominated by the circumbinary envelope rather than by the individual disks around the protostars. This is not particularly surprising since the individual circumstellar disks are expected to be heavily tidally truncated in this very compact binary system (projected separation of order 40 AU). In contrast, the continuum at 7 mm is dominated by free-free radiation from the bases of the thermal jets and enables us to pin-point the embedded sources A1 and A2 (Figure 2). This demonstrates the complementarity of ALMA and the VLA to study young stellar sources.

When it is reconstructed to optimize sensitivity, the 7 mm emission from source A also reveals a faint elongation toward the NE similar to that seen in the sub-millimeter map, and extended emission surrounding the sources A1 and A2. Like the sub-millimeter continuum, this extended emission likely traces the circumbinary envelope. The emission associated with the extension of source A to the north-east (i.e. with source Ab from Chandler et al. 2005) contributes roughly 1.4 mJy at 41 GHz, 0.5 Jy at 305 GHz (Chandler et al. 2005) and 3 Jy at 696 GHz (all values with relative uncertainties of order 50%). This yields a spectral index of 2.7 $\pm$ 0.5, consistent with that of the more compact emission from source A (Chandler et al. 2005). We argue that this elongation traces faint extended emission from the circumbinary envelope (possibly related to dust accumulated in that direction by the NE-SW flow), rather than a new protostellar source in the system.

Both the 7 mm and the 4 cm continuum maps (Figure 2) reveal a new compact source to the NE of source A2. This is strikingly similar to the situation encountered in the 2006 image of IRAS 16293–2422 at λ = 1.3 cm (Loinard et al. 2007) when a bipolar ejection from A2 was seen for the first time. The bipolar ejection that occurred in 2006 produced the sources A2α and A2β that are still clearly seen in the 4 cm image (Figure 2c) and, faintly, in the 7 mm map (Figure 2a). They are moving away from A2 at projected velocities of several tens of km s^{-1} (Pech et al. 2010). We interpret the new source to the NE of A2 (which we shall call A2δ) as a new ejection from A2. In the high resolution 7 mm image, there is a faint extension to the SW of A2 which might correspond to the bipolar counterpart of A2δ. We note that in the first image following the ejection of the A2α/A2β pair (Loinard et al. 2007), the SW ejecta (A2α) was not immediately detached from A2 either.

IRAS 16293–2422 has been regularly monitored at centimeter wavelengths since the late 1980s (Chandler et al. 2005) and the 2006 ejection was the first to be detected. The new ejection reported here suggests that source A2 might be entering a period of enhanced outflow activity. Regular observations in the coming years and decades will be required to confirm this possibility, and will enable a detailed study of the kinematics and behavior of the ejecta. Interestingly, A2α, A2β, A2δ, and A2 itself are well aligned (Figure 2c) but the position angle ($\sim$ 70°) of the line joining them is somewhat larger than the position angle ($\sim$ 55°) of the large-scale outflow known to originate from A2 (e.g. Figure 5 in Mizuno et al. 1990). This suggests that the jet driven by source A2 is precessing as a consequence of the A1-A2 binarity. We note, finally, that there is no detectable CO(6-5) emission associated with the NE-SW flow in the ALMA observations (Figure 3). This is in agreement with the results of Yeh et al. (2008) who also failed to detect such emission in their SMA CO observations at arcsecond resolution.

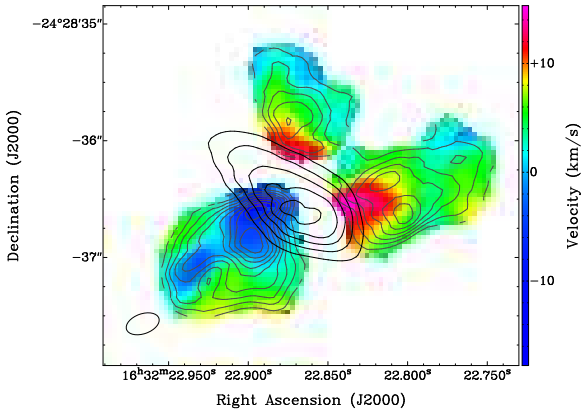

Figure 3. Integrated intensity of the weighted velocity (moment 1) color map of the CO(6-5) emission from source A overlaid in contours with the 0.45 mm continuum emission (black thick line) and the integrated intensity line emission (moment 0) of the CO(6-5) (grey thin line). The black contours are the same as in Figure 1 (0.2 to 1.2 Jy beam^{-1} in steps of 0.2 Jy beam^{-1}). The grey contours are from 10% to 90% with steps of 10% of the peak of the CO line emission; the peak is 3.2 $\times$ 10^4 Jy Beam^{-1} km s^{-1}. The color-scale bar on the right indicate the LSR velocities in km s^{-1}. The synthesized beam of the continuum image is shown in the bottom left corner of the image.

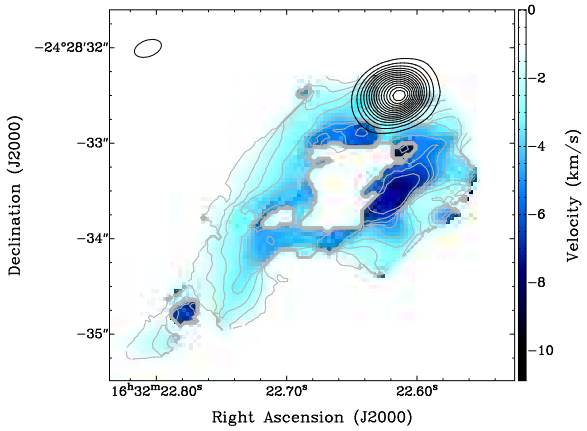

Figure 4. Integrated intensity of the weighted velocity (moment 1) color map of the CO(6-5) emission from source B overlaid in contours with the 0.45 mm continuum emission (black thick line) and the velocity scale of the CO(6-5) (grey thin line). The black contours are the same as in Figure 1 (starting at and in step of 0.2 Jy beam^{-1}). The color-scale bar on the right indicate the LSR velocities in km s^{-1}. The synthesized beam of the continuum image is shown in the upper left corner of the image.

3.2 The EW flow

Strong CO(6-5) is detected in the ALMA data around the position of source A. In agreement with the results of Yeh et al. (2008), it is largely concentrated to an EW structure with blueshifted emission to the east and redshifted emission to the west; This emission traces the central part of the well-known EW (PA $\sim$ 110°) flow (Figure 3). In spite of the high angular resolution of the ALMA observations, the origin of the flow stall cannot be traced back to a specific source within component A.

3.3 A compact outflow from source B

As reported by Yeh et al. (2008) and confirmed by Rao et al. (2009), there is very strong blue-shifted CO emission to the south of source B (the location of component b2 in Yeh et al. 2008). Figure 4 displays the first moment CO(6-5) map of this component (in colors) overlaid with the 0.45 mm continuum image (in contours). It is clear that the CO emission defines a 3″-long bubble-like structure oriented along the south-east–north-west direction (at P.A. $\sim$ 130°) with source B at its north-west apex. This structure points from source B toward source A, but there appears to be no material connection (i.e. no bridge of emission) between the two. In particular, its south-east apex (corresponding to the point nearest to A) is located about 2″ to the north-west of source A. We conclude that this structure is associated with source B, and unrelated to source A. We should point out, here, that there is a significant amount of extended CO emission around the systemic velocity of IRAS 16293–2422 ($v_{lsr} \sim 4$ km s^{-1}) in the ALMA observations. This emission is poorly recovered by the interferometer, and its structure cannot be assessed; we filtered it out by ignoring the velocity channels around 4 km s^{-1}, but note that our fluxes (as given, for instance, in Figure 4) are clearly underestimated since they do not include the ambient gas. Interestingly, Rao et al. (2009) recently reported on the possible detection of a new outflow in IRAS 16293–2422 seen in SiO(8-7) along a position angle very similar to that of the CO structure seen here. The structure seen in SiO, however, is most prominent south of source A, and entirely at positive velocities. While there is SiO(8-7) emission in the general direction of the CO structure reported here, it is at +4 km s^{-1} rather than at –4 km s^{-1}. Higher resolution SiO observations will clearly be needed to establish the relation (if there is any) between the SiO structure reported by Rao et al. (2009) and the CO structure reported here.

To our knowledge, ours is the first direct indication for the existence of an outflow driven by source B. Interestingly, there is no strong redshifted counterpart to the north-west. While this might reflect an intrinsic asymmetry of the flow, it could also at least partly reflect the structure of the circumstellar environment. As discussed by Pineda et al. (2012) and Zapata et al. (in prep.), at sub-millimeter wavelengths, both the CO lines and the continuum emission toward source B are optically thick, so the red-shifted emission might be at least partly hidden from view. Alternatively, IRAS 16293–2422 might be located close to the back side of the cloud where it is located. Besides explaining the lack of a red-shifted lobe, this would be consistent with the very high optical depth toward source B.

Since the systemic velocity of source B is about 3 km s^{-1} (Jørgensen et al. 2011) while the most negative velocities reached by the outflow are $\sim$ –8 km s^{-1}, the (radial) expansion velocity of the bubble relative to source B is about 10 km s^{-1}. At the distance of Ophiuchus, the angular extent of the bubble (3″) corresponds to 5.4 $\times$ 10^{15} cm (360 AU), and the dynamical age of the flow is of order 200 years. While this calculation might only provide a crude estimate of the true age of the structure, similar calculations for the other outflows in the system (Mizuno et al. 1990) yield much larger dynamical ages, of order 10^4 years. This is consistent with the commonly held view that source B is the youngest object in IRAS 16293–2422 (e.g. Chandler et al. 2005). It could be argued that the true angular extent of the outflow is significantly larger than reported here, because the CO(6-5) line might only pick the most highly excited gas in the vicinity of source B. This is unlikely because lower J CO observations (e.g. Yeh et al. 2008) did not reveal any conspicuous emission on larger scales along the direction of this structure.

The 7 mm continuum emission around source B has usually been interpreted as a nearly face-on disk (Rodríguez et al. 2005). Recent ALMA spectroscopic observations further revealed unam-

biguous evidence for infall and rotation (Pineda et al. 2012, Zapata et al. in prep.) toward that source, and the rotation is also consistent with a nearly face-on orientation. In this configuration, the flow driven by source B ought to be oriented nearly along the line of sight, and the expansion velocity would be mostly radial. This suggests that the true expansion velocity of the flow is not significantly larger than the observed 10 km s^{-1}.

The overall morphology of the outflow driven by source B is qualitatively different from that of typical flows powered by low-mass young stars. In particular, there is no evidence for a collimated jet-like structure along the symmetry axis. Instead, the highest (i.e. most negative) velocities are associated with the inner layer of the structure, while the outer layers are at less negative velocities (typically at about −2 km s^{-1}; see Figure 4). This behavior suggests that source B drives a moderately collimated wind, that impinges into the stationary circumstellar medium, in a situation resembling that described theoretically by Shu et al. (1991).

In summary, the flow driven by source B has a number of peculiar properties. It is fairly slow ($\sim$ 10 km s^{-1}), outburst-like, and only moderately collimated. Those are characteristics theoretically expected from flow driven by adiabatic (first) cores (Machida et al. 2008, Price et al. 2012; see also Chen et al. 2010, Enoch et al. 2010, Dunham et al. 2011, Pineda et al. 2011 for observational aspects). However, the evidence for strong accretion reported by Pineda et al. (2012) and Zapata et al. (in prep.) and the fact that component B is such a bright submillimeter continuum source would be more consistent with the idea that it has already entered the protostellar phase. In any case, the properties of the outflow driven by this object do suggest that it might be one of the youngest known protostars.

4 CONCLUSIONS AND PERSPECTIVES

In this *Letter*, we used combined ALMA and VLA observations to examine the outflow activity in the very young (Class 0) protostellar system IRAS 16293–2422. The well-known NE-SW and E-W large-scale molecular flows are confirmed to be driven from within component A to the south-east of the system. The NE-SW flow can unambiguously be associated with source A2 which might be entering a phase of enhanced activity. The ALMA CO(6-5) observations have enabled us to discover a new outflow toward source B with peculiar properties: it is highly asymmetric, resembles an outburst, is fairly slow (10 km s^{-1}), and lacks a jet-like feature along its symmetry axis. In addition, its dynamical age is only about 200 years. We argue that these properties result from the extreme youth of source B, which might be one of the youngest known protostars. Given the short dynamical age of the structure, significant morphological changes are expected to take place over the next few decades. Observing this time evolution would help constrain the formation and early evolution of molecular outflows in general, and would have a fundamental impact on our understanding of these objects.

ACKNOWLEDGMENTS

L.L., L.A.Z., L.F.R. and G.P. acknowledge the support of DGAPA, UNAM, and of CONACyT (México). LL is indebted to the Alexander von Humboldt Stiftung for financial support. BP is supported by the DFG Emmy Noether grant PA1692/1-1. The National Radio Astronomy Observatory is a facility of the National Science Foundation operated under cooperative agreement by Associated Universities, Inc. This paper makes use of the following ALMA data: ADS/JAO.ALMA#2011.0.00007.SV. ALMA is a partnership of ESO (representing its member states), NSF (USA) and NINS (Japan), together with NRC (Canada) and NSC and ASIAA (Taiwan), in cooperation with the Republic of Chile. The Joint ALMA Observatory is operated by ESO, AUI/NRAO and NAOJ.

REFERENCES

Arce, H. G., Shepherd, D., Gueth, F., et al. 2007, Protostars and Planets V, 245
Bodenheimer, P. 1995, ARAA, 33, 199
Carrasco-González, C., Anglada, G., Rodríguez, L. F., et al. 2008, ApJ, 676, 1073
Castets, A., Ceccarelli, C., Loinard, L., Caux, E., & Lefloch, B. 2001, A&A, 375, 40
Ceccarelli, C., Castets, A., Caux, E., et al. 2000, A&A, 355, 1129
Chandler, C. J., Brogan, C. L., Shirley, Y. L., & Loinard, L. 2005, ApJ, 632, 371
Chen, X., Arce, H. G., Zhang, Q., et al. 2010, ApJ, 715, 1344
Crimier, N., Ceccarelli, C., Maret, S., et al. 2010, A&A, 519, A65
Dunham, M. M., Chen, X., Arce, H. G., et al. 2011, ApJ, 742, 1
Enoch, M. L., Lee, J.-E., Harvey, P., Dunham, M. M., & Schnee, S. 2010, ApJ, 722, L33
Gooch, R. 1996, Astronomical Data Analysis Software and Systems V, 101, 80
Hirano, N., Mikami, H., Umemoto, T., Yamamoto, S., & Taniguchi, Y. 2001, ApJ, 547, 899
Jørgensen, J. K., Bourke, T. L., Nguyen Luong, Q., & Takakuwa, S. 2011, A&A, 534, A100
Jørgensen, J. K., Favre, C., Bisschop, S. E., et al. 2012, ApJ, 757, L4
Lada, C. J. 1985, ARAA, 23, 267
Loinard, L. 2002, RevMexAA, 38, 61
Loinard, L., Chandler, C. J., Rodríguez, L. F., et al. 2007, ApJ, 670, 1353
Loinard, L., Torres, R. M., Mioduszewski, A. J., & Rodríguez, L. F. 2008, ApJ, 675, L29
Machida, M. N., Inutsuka, S.-i., & Matsumoto, T. 2008, ApJ, 676, 1088
Mizuno, A., Fukui, Y., Iwata, T., Nozawa, S., & Takano, T. 1990, ApJ, 356, 184
Mundy, L. G., Wootten, A., Wilking, B. A., Blake, G. A., & Sargent, A. I. 1992, ApJ, 385, 306
Pech, G., Loinard, L., Chandler, C. J., et al. 2010, ApJ, 712, 1403
Pineda, J. E., Maury, A. J., Fuller, G. A., et al. 2012, A&A, 544, L7
Pineda, J. E., Arce, H. G., Schnee, S., et al. 2011, ApJ, 743, 201
Price, D. J., Tricco, T. S., & Bate, M. R. 2012, MNRAS, 423, L45
Rao, R., Girart, J. M., Marrone, D. P., Lai, S.-P., & Schnee, S. 2009, ApJ, 707, 921
Reipurth, B., Bally, J., & Devine, D. 1997, AJ, 114, 2708
Rodríguez, L. F., Loinard, L., D'Alessio, P., Wilner, D. J., & Ho, P. T. P. 2005, ApJ, 621, L133
Shu, F. H., Ruden, S. P., Lada, C. J., & Lizano, S. 1991, ApJ, 370, L31
Walker, C. K., Lada, C. J., Young, E. T., Maloney, P. R., & Wilking, B. A. 1986, ApJ, 309, L47
Wootten, A. 1989, ApJ, 337, 858
Yeh, S. C. C., Hirano, N., Bourke, T. L., et al. 2008, ApJ, 675, 454